minerals

MDPI

Review

New Data on the Isomorphism in Eudialyte-Group Minerals. 2. Crystal-Chemical Mechanisms of Blocky Isomorphism at the Key Sites

Ramiza K. Rastsvetaeva [1] and Nikita V. Chukanov [2,3,*]

[1] Shubnikov Institute of Crystallography of Federal Scientific Research Centre "Crystallography and Photonics", Russian Academy of Sciences, Leninskiy Prospekt 59, 119333 Moscow, Russia; rast@crys.ras.ru
[2] Institute of Problems of Chemical Physics, Russian Academy of Sciences, Chernogolovka, 142432 Moscow, Russia
[3] Faculty of Geology, Moscow State University, Vorobievy Gory, 119991 Moscow, Russia
* Correspondence: nikchukanov@yandex.ru

Received: 24 July 2020; Accepted: 14 August 2020; Published: 17 August 2020

Abstract: The review considers various complex mechanisms of isomorphism in the eudialyte-group minerals, involving both key positions of the heteropolyhedral framework and extra-framework components. In most cases, so-called blocky isomorphism is realized when one group of atoms and ions is replaced by another one, which is accompanied by a change in the valence state and/or coordination numbers of cations. The uniqueness of these minerals lies in the fact that they exhibit ability to blocky isomorphism at several sites of high-force-strength cations belonging to the framework and at numerous sites of extra-framework cations and anions.

Keywords: eudialyte group; crystal chemistry; blocky isomorphism; peralkaline rocks

1. Introduction

Eudialyte-group minerals (EGMs) are typical components of some kinds of agpaitic igneous rocks and related pegmatites and metasomatic assemblages. Crystal-chemical features of these minerals are important indicators reflecting conditions of their formation (pressure, temperature, fugacity of oxygen and volatile species, and activity of non-coherent elements [1–9]).

A unique crystal-chemical diversity of EGMs is determined by a wide variability of their chemical composition involving more than 30 main elements and complex mechanisms of homovalent, heterovalent, and, especially, blocky isomorphism involving groups of atoms having different valency and coordination. The uniqueness of these minerals lies in the fact that they exhibit ability to blocky isomorphism at several sites of high-force-strength cations belonging to the framework and at numerous sites of extra-framework cations and anions.

According to the recommendation of the Commission on New Minerals, Nomenclature, and Classification of the International Mineralogical Association [3], the general formula of EGMs is $N1_3N2_3N3_3N4_3N5_3M1_6M2_{3-6}M3M4Z_3(Si_{24}O_{72})Ø_{4-6}X_2$. In this formula, most symbols denote split sites (i.e., groups of closely spaced sites). The "rigid" part of the structures of eudialyte-type minerals (Figure 1) is a 3D quasi-framework consisting of the $^{IV}Si_3O_9$, $^{IV}Si_9O_{27}$, and $^{VI}M1_6O_{24}$ rings ($M1$ = Ca, Mn^{2+}, Fe^{2+}, Na, *Ln*, Y, Sr; coordination numbers are denoted by Roman numerals) connected via $M2O_{4-7}$ polyhedra and ZO_6 octahedra ($M2$ = Fe^{2+}, Fe^{3+}, Mn^{2+}, Mn^{3+}, Mg, Zr, Ta, Na; Z = Zr, Ti, Nb) and containing additional $M3$ and $M4$ sites which are situated at the centers of two nonequivalent Si_9O_{27} rings and can be occupied by ^{IV}Si, ^{VI}Nb, ^{VI}Ti, and ^{VI}W, as well as subordinate Al, Na, and other components whose charges vary from +1 to +6 [1,2] (Figure 1). In the structures of most EGMs, including eudialyte *s.s.*, $M1$ cations can be disordered, but in some representatives of this mineral group

they alternate in the ring of octahedra, which results in its transformation into the ring ($M1.1_3M1.2_3O_{24}$) and symmetry lowering from the space group *R*3*m* or *R*-3*m* to *R*3. In some samples, a splitting of the *M*1 site [10] or one of the *M*1.1/*M*1.2 sites [11] into two sub-sites located at short distance of ~0.2 Å from each other takes place. The *M*1–*M*4 sites are considered as the main species-defining "key sites" in the nomenclature of EGMs [3,6,7,12,13].

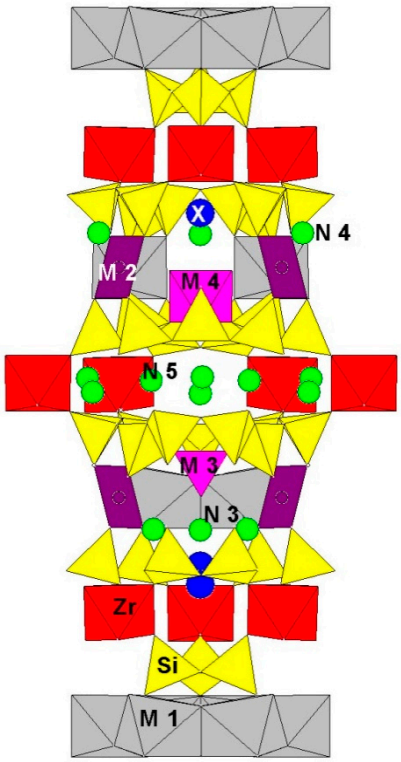

Figure 1. Arrangement of key sites in the eudialyte-type structures viewed along (210).

Extra-framework cations (Na^+, K^+, Ca^{2+}, Mn^{2+}, Sr^{2+}, Ba^{2+}, Pb^{2+}, Y^{3+}, Ln^{3+}, and H_3O^+) and (in some samples) water molecules occupy five sites, *N*1–*N*5, which are typically split and can be partly vacant. Cations other than Na^+ show a tendency to concentrate at the *N*3 and *N*4 sites. Some of these cations (K^+, Ca^{2+}, Mn^{2+}, Sr^{2+}, Ce^{3+}, and H_3O^+) are species-defining ones in several representatives of the eudialyte group. The Ø anions (Ø = O, OH) coordinate the *M*2, *M*3, and *M*4 sites. Additional anions (Cl^-, F^-, OH^-, S^{2-}, SO_4^{2-}, and CO_3^{2-}) and water molecules occur at the *X*1 and *X*2 sites located on the three-fold axis.

Blocky isomorphism is defined as the ability of groups of atoms or ions having different configurations to replace each other in crystal structures [14]. Such substitutions are known for a large number of alkaline zircono- and titanosilicates [9]. In EGMs this kind of isomorphism is realized at the key sites *M*2, *M*3, and *M*4, as well as at the *N* and *X* sites. The eudialyte group is the only group of minerals in which blocky isomorphism is realized at several sites containing high-force-strength cations. Below we will use the symbols *N*1–*N*5, *M*2, *M*3, *M*4, and *X* to denote corresponding cavities (i.e., micro-regions which can contain several closely spaced sites).

In addition to EGMs with the rhombohedral unit-cell parameters $a \sim 14.2$ Å, $c \sim 30$ Å, members of the eudialyte group with modular structures and doubled *c* parameter are known. Their unit cells contain two eudialyte-type modules which differ from each other by local situations around key sites [4].

2. Blocky Isomorphism at the *M*2 Site

The most complex blocky isomorphism is realized in the *M*2 micro-region situated between rings of octahedra, $M1_6O_{24}$ [15]. This micro-region can be populated by cations having different radii, charges, and coordination (from flat square formed by edges of octahedra belonging to two neighboring $M1_6O_{24}$ rings to a 7- or 8-fold polyhedron): $^{IV}Fe^{2+}$, $^{V}Fe^{2+}$, $^{V}Fe^{3+}$, $^{VI}Fe^{3+}$, $^{V}Mn^{2+}$, $^{VI}Mn^{2+}$, ^{IV}Zr, ^{IV}Ta, ^{IV}Na, ^{V}Na, ^{VI}Na, ^{VII}Na, ^{VI}K, ^{VII}K, and ^{VIII}K. The *M*2-cations occur in the plane of the six-membered rings which is perpendicular to the threefold axis (Figure 2). The coordination polyhedra $M2O_5$ and $M2O_7$ can have different orientations with respect to the plane of the square. Some examples of *M*2-centered polyhedra are shown in Figure 3.

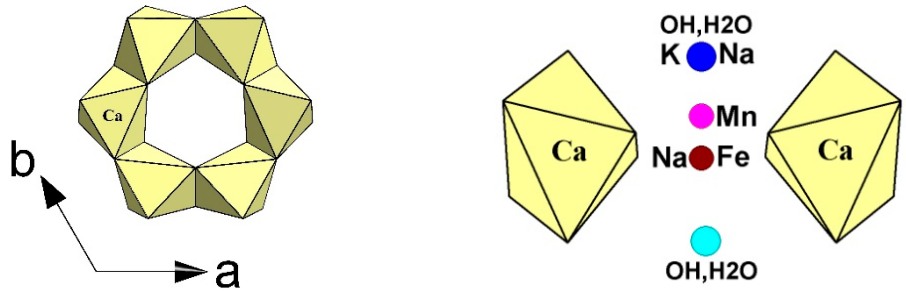

Figure 2. Six-membered ring composed of *M*1 octahedra (**a**) and positions of some components in the *M*2 micro-region between neighboring rings of *M*1 octahedra (**b**).

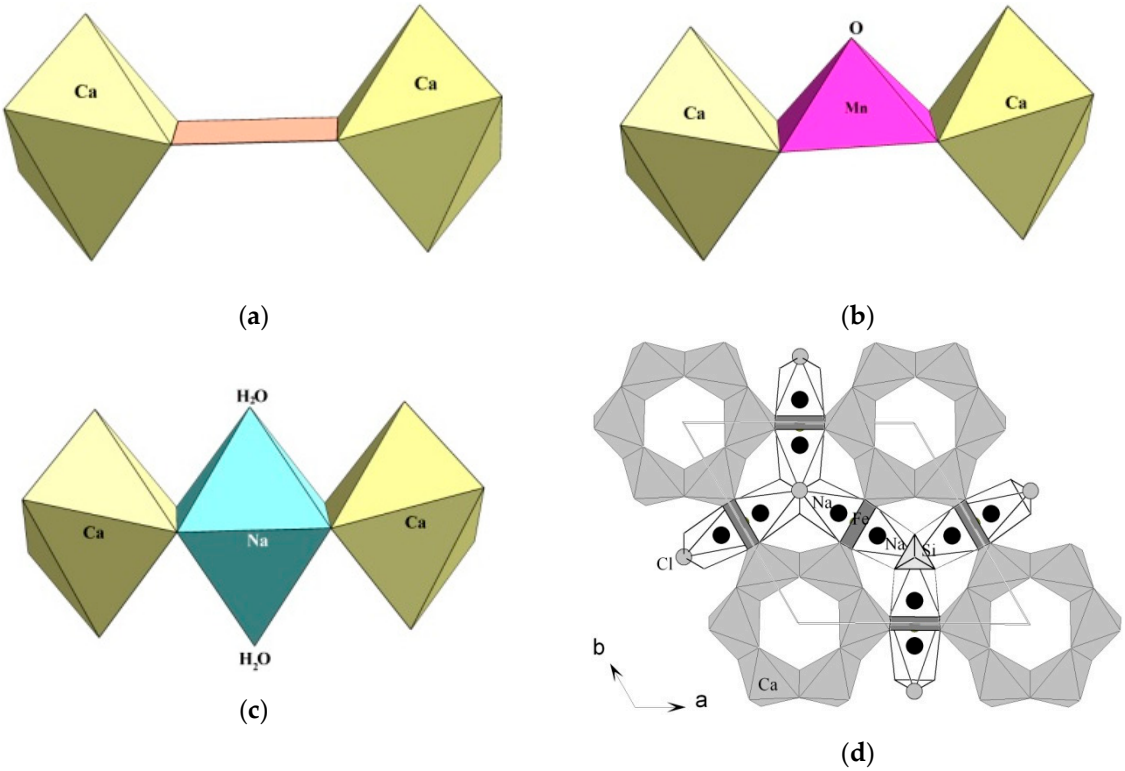

Figure 3. Different polyhedra in the structures of eudialyte-group minerals: square (**a**), tetragonal pyramid (**b**), and octahedron (**c**), all viewed along (210), and the arrangement of 7-fold ^{M2}Na-centered polyhedra in a high-sodium EGM [28] (**d**).

The fourfold (nearly, flat-square) coordination is most typical for Fe^{2+} and, to a less extent, for Na. In particular, eudialyte *s.s.* is $^{M2}(^{IV}Fe^{2+})$-dominant [16,17]. The crystal structures of $^{M2}(^{IV}Na)$-dominant

minerals are described in [11,18–24]. Some other components (Zr, Hf, and Ta) can occur in the $M2O_4$ polyhedron in subordinate amounts [1]. The mean *M*2–O distances vary from 2.04 Å for *M*2 = Fe^{2+} to 2.29 Å for *M*2 = Na (Table 1).

Table 1. Geometric parameters of the $M2O_4$ polyhedra for different cations.

Cation	*M*2–O Distances, Å (Ranges)	O–O Distances, Å	Reference
Na^+	2.29–2.29	3.28, 3.28, 3.13 × 2	[22]
Zr^{4+}	2.040–2.117	2.78, 2.81, 3.03, 3.08	[25]
Ta^{5+}	2.035–2.116	2.95, 3.11, 2.85 × 2	[26]
Fe^{2+}	2.03–2.06	2.95, 2.98, 2.80 × 2	[27]

The fivefold *M*2-centered polyhedron is a square pyramid $M2O_4Ø$ (Figure 3) where O atoms belong to the neighboring $M1_6O_{24}$ rings and Ø is OH group of the $M3O_3(OH)_3$ or $M4O_3(OH)_3$ octahedron or H_2O molecule. Kentbrooksite $(Na,REE)_{15}(Ca,REE)_6{}^{V}Mn^{2+}{}_3Zr_3[SiNb](Si_{24}O_{74})F_2{\cdot}2H_2O$ (Figure 4a) was the first EGM in which such polyhedron was identified [29]. Later, $^{V}M2$ site was found in different EGMs [30–48]. Mn-dominant $^{V}M2$ site occurs in the structure of andrianovite [30,31]. In the ilyukhinite structure [47,48] the *M*2 site has a fourfold flat-square coordination with the *M*2–O distances of 2.11–2.51 Å and is predominantly occupied by Mn with a minor Fe admixture. The replacement of manganese with iron at the fivefold *M*2 site has been established in a number of minerals close in structure to kentbrooksite including ferrokentbrooksite [32], georgbarsanovite [33,34], taseqite [35,36], feklichevite [37], golyshevite [38,39], as well as some varieties of other EGMs [1]. In the *M*2 micro-region of so-called "eucolite" (a variety of ferrokentbrooksite [40]), Fe atoms occupy two sites located at the distance of 0.49 Å from each other and having a joint occupancy about 100%. In most cases, differently oriented square pyramids occur in the *M*2 micro-region [1,41–43]. In siudaite [49], the *M*2 site is split into the *M*2a and *M*2b sub-sites which are located on both sides from the *M*2 square at the distance of 0.99 Å from each other and have fivefold square pyramid coordination. The population of the $M2aO_4Ø$ and $M2aO_4Ø$ polyhedra (Ø = O, OH) is $Fe^{3+}{}_{0.4}Mn^{2+}{}_{0.4}$ and $Fe^{3+}{}_{0.2}$, respectively. This conclusion was confirmed by means of Mössbauer spectroscopy. In some EGMs, $M2O_4Ø_2$ octahedra (Figure 3) are formed involving OH groups (or H_2O) situated on both sides from the $M2O_4$ square where *M*2 is Mn^{2+} (in manganoeudialyte) or Fe^{3+} (in ikranite: Figure 4b).

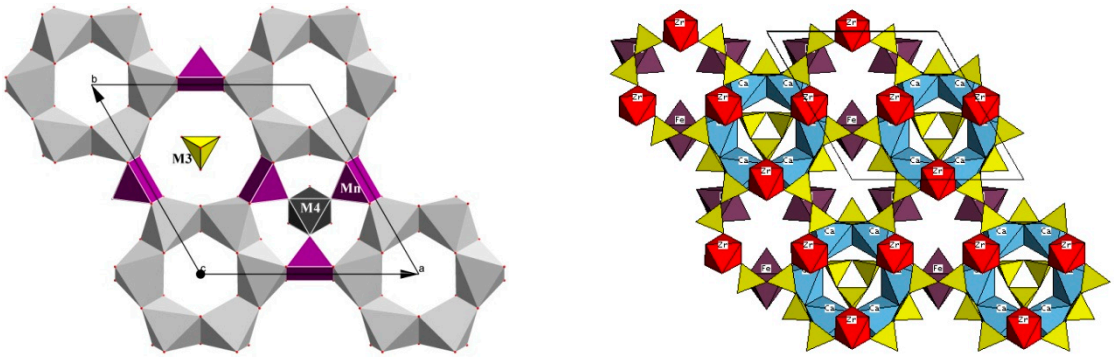

(**a**) (**b**)

Figure 4. Fragments of the crystal structures of kentbrooksite (**a**) and ikranite (**b**) viewed along (001).

The $^{VII}M2$-centered sevenfold polyhedra are based on the flat square and include O atoms of the framework and large *X* anions. Positions of large cations (K^+, Sr^{2+}, or Ce^{3+}) occurring in the *M*2 micro-region, are located at large distances from the plane of the O_4 square. In these cases, the coordination polyhedron is supplemented by two inner O atoms of the Si_9O_{27} ring and one or two

(statistically) species anions (Cl, F, or H_2O) situated at the *X* site on the threefold axis. As a result, a 7- or 8-fold polyhedron is formed. The coordination number of Na^+ occurring in the *M*2 micro-region can vary from 4 to 7. The ^{VII}Na-centered polyhedron dominates in the *M*2 micro-region of some samples [28,44]. As a subordinate component, $^{M2}(^{VII}Na)$ occurs in the structures of intermediate members of the manganoeudialyte–ilyukhinite [45] and eudialyte–sergevanite [46] solid-solution series, with the Na–O distances of 2.23(4)–2.96(3) and 2.33(1)–3.01(1) Å, respectively. Rarely, the $^{VII}M2$ polyhedron is centered by Mn or Zr.

3. Blocky Isomorphism at the *M*3 and *M*4 Sites

The micro-regions *M*3 and *M*4 at the centers of two nonequivalent Si_9O_{27} rings can be vacant, but usually they contain tetrahedra (SiO_4, rarely AlO_4) or octahedra (typically, NbO_6; rarely, TiO_6, WO_6, MnO_6, and NaO_6) [1] (Figure 5). The positions of *M*3 and *M*4 cations are located on the threefold axis, and their charge can vary from +1 (Na) to +6 (W). When SiO_4 tetrahedron occurs in the *M*3 or *M*4 micro-region, corresponding Si_9O_{27} ring transforms into a 10-membered disc consisting of three 5-membered rings (Figure 5b).

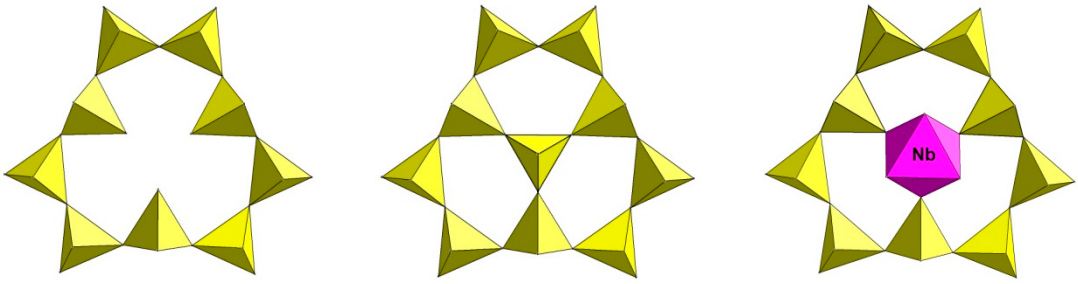

Figure 5. Local situations at the centers of the Si_9O_{27} rings viewed along (001). (**a**) A ring with vacancy at the *M*3 site, (**b**) a ring centered with the SiO_4 tetrahedron, (**c**) a ring centered with the NbO_6 octahedron.

Three O atoms which form the base of each Si-centered tetrahedron occurring in the *M*3 or *M*4 micro-region are common with O atoms of the Si_9O_{27} ring. The fourth O atom of this tetrahedron belongs to OH group. The ^{M3,M4}Si atoms can occur either above or below the triangular base of the tetrahedron, and OH groups belonging to the tetrahedra can be located on both sides of the Si_9O_{27} ring in such a way that apical vertices of the neighboring tetrahedra are oriented in opposite directions. Different options involving *M*3 and *M*4 tetrahedra are shown in Figure 6. It is to be noted that the *M*3a and *M*3b tetrahedra, as well as *M*4a and *M*4b tetrahedra cannot exist in corresponding micro-regions simultaneously because of short ^{M3a}Si–^{M3b}Si and ^{M4a}Si–^{M4b}Si distances. The option (b) corresponds to a centrosymmetric structure, and the options (d) and (e) correspond to non-centrosymmetric ones.

The option (c) is most common, but corresponding local situation cannot be realized due to unacceptably short OH–OH distance of 1.4–1.5 Å between the vertices of the tetrahedra. However, this option can be realized statistically.

An example of the option (a) is the crystal structure of a high-silicon EMG from the Kovdor massif, Kola Peninsula, described as "low-iron eudialyte 2" [50]. In this sample, the *M*3 and *M*4 sites occupied by Si are split into pairs of partially occupied sub-sites located at short distances from each other: *M*3a–*M*3b = 0.92(6) Å and *M*4b–*M*4c = 1.04(1) Å. As noted above, a local situation when both *M*3b and *M*4a sites are occupied is impossible due to a short distance (of 1.41 Å) between OH groups belonging to corresponding tetrahedra.

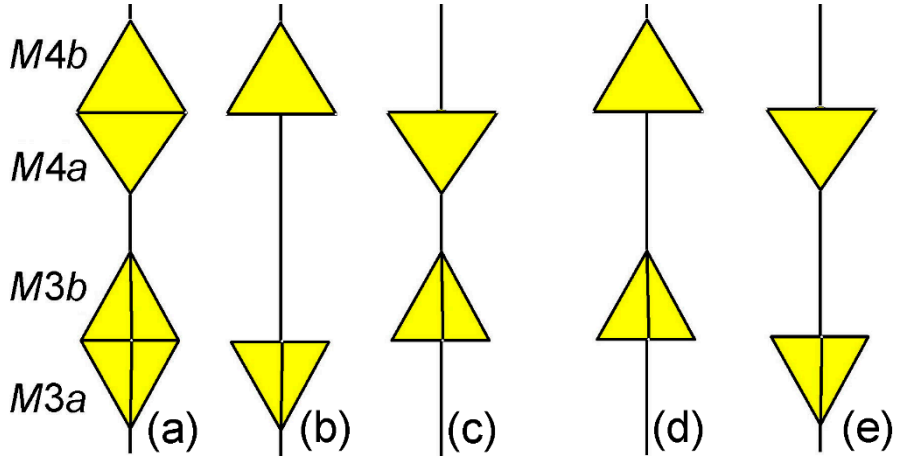

Figure 6. (**a**–**e**) A scheme showing different options of mutual orientation of the *M*3 and *M*4 tetrahedra.

Our investigations carried out on a large selection of EGMs [5,51] (Table 2) have shown that the total amount of Si atoms at the *M*3 and *M*4 sites ($\sum T$) varies in wide ranges, from 0.88 to almost 2 atoms per formula unit (*apfu*) ($Z = 3$). The ratio of the amounts of differently oriented tetrahedra ($\sum T_a/\sum T_b$) varies from 0 to 2.31; only in two structures this ratio is equal to 1 which corresponds to the existence of center of symmetry. Both centrosymmetric structures are characterized by rather low $\sum T$ values of 1.12 and 1.39 *apfu*, and only one of them corresponds to the option (a).

Table 2. Population of tetrahedral sites in the *M*3 and *M*4 micro-regions, total amounts of the $^{IV}M3$ and $^{IV}M4$ components ($\sum T$, $Z = 3$) and atomic ratios of the contents of ($^{IV}M3$a,$^{IV}M4$a) and ($^{IV}M3$b,$^{IV}M4$b) cations ($\sum T_a/\sum T_b$). The samples are listed in the order of lowering of the $\sum T$ value.

No.	Mineral	*M*3a	*M*3b	*M*4a	*M*4b	$\sum T$	$\sum T_a/\sum T_b$	References
1.	Davinciite	0.5Si	0.49Si	0.41Si	0.53Si + 0.04Al	1.97	0.86	[52,53]
2.	Fe-poor EGM	0.1Al	0.4Si + 0.5Mn		0.9Si	1.9	0.05	[41]
3.	Fe-poor EGM	0.24Si	0.57Si	0.48Si	0.47Si	1.76	0.69	[50]
4.	H_3O-analogue of eudialyte	0.45Si	0.34Si	0.57Si	0.21Si + 0.19Al	1.76	1.38	[19]
5.	Aqualite	0.45Si	0.55Si	0.5Si		1.72	2.13	[21,54,55]
6.	Ta-bearing eudialyte		0.5Si + 0.3Al	0.43Si	0.35Si	1.58	0.37	[26]
7.	Sergevanite	0.55Si		0.51Si	0.49Si	1.55	2.16	[44]
8.	Sergevanite	0.5Si	0.5Al		0.5Si	1.5	0.5	[25,56]
9.	Raslakite	0.4Si + 0.1Al		0.4Si + 0.1Al	0.5Si	1.5	2.0	[42,57]
10.	H_3O-analogue of eudialyte		0.44Si + 0.06Al	0.5Si	0.5Si	1.5	0.5	[19]
11.	Mangano-eudialyte	0.38Si	0.25Al	0.37Si	0.44Si	1.44	1.09	[58]
12.	H_3O-analogue of eudialyte	0.29Si	0.2Si	0.41Si	0.49Si	1.39	1.01	[19]
13.	Taseqite		0.3Si		1.0Si	1.3	0	[35,36,59–61]
14.	Na-rich eudialyte	0.56Si			0.56Si	1.12	1.0	[28]

Table 2. *Cont.*

No.	Mineral	*M*3a	*M*3b	*M*4a	*M*4b	$\sum T$	$\sum T_a/\sum T_b$	References
15.	H_3O-rich and Si-deficient EGM	0.5Si	0.31Si	0.07Al	0.17Si	1.05	1.19	[19]
16.	H_3O-rich and Si-deficient EGM	0.44Si	0.1Al	0.23Si	0.19Si	0.96	2.31	[19]
17.	Andria-novite			0.2Si	0.75Si	0.95	0.27	[30,31]
18.	H_3O-rich and Si-deficient EGM	0.18Si + 0.2Al			0.5Si	0.88	0.76	[19]

In Si-deficient EGMs, the *M*3 and *M*4 micro-regions contain vacancies (as e.g., in ikranite [57,62,63] and mogovidite [38,64]) and/or octahedra formed by three O atoms common with the Si_9O_{27} rings and three OH groups. The *M*3 and *M*4 cations with octahedral coordination can occur in one of three sites located at short distances from the $^{IV}M3$ and $^{IV}M4$ sites which are usually occupied by Si. Consequently, the $^{IV}M3$ and $^{VI}M3$ sites, as well as the $^{IV}M4$ and $^{VI}M4$, cannot be occupied simultaneously in the same micro-region. In most cases, blocky isomorphism involving atoms with tetrahedral and octahedral coordination is realized in the *M*3 and *M*4 micro-regions. However, there are cases when these microregions contain only one type of polyhedra, namely, only tetrahedra (for example, in davinciite [52,53]), or only octahedra. The latter case is realized in the centrosymmetric high zirconium eudialyte described by Giuseppetti [65], in which the *M*3 and *M*4 sites have been refined with the same occupancy, $\square_{0.65}{}^{VI}Zr_{0.35}$. However, the possibility of the occurrence of Zr in the *M*3 and *M*4 micro-regions was not confirmed by subsequent investigations. In most cases, octahedral sites in these micro-regions are occupied by Nb. In three EGMs (khomyakovite and manganokhomyakovite [66], and johnsenite-(Ce) [67]) the $^{VI}M3$ site is occupied by W. Some examples of blocky isomorphism in the *M*3 and *M*4 micro-regions are presented in Figures 7–9.

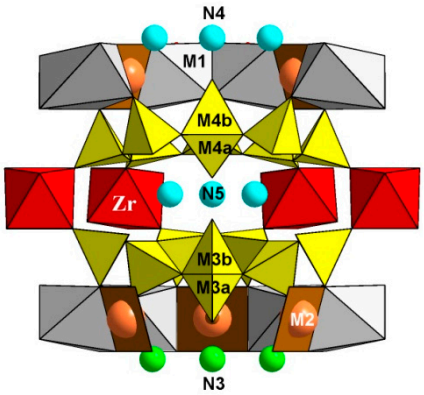

Figure 7. A fragment of the crystal structure of davinciite.

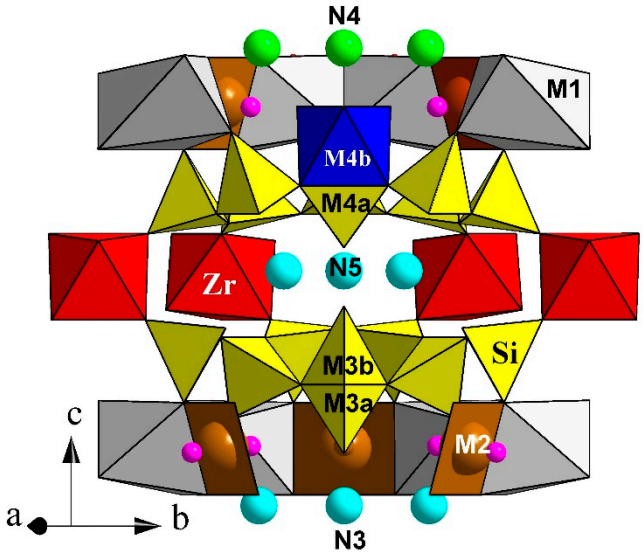

Figure 8. A fragment of the crystal structure of andrianovite.

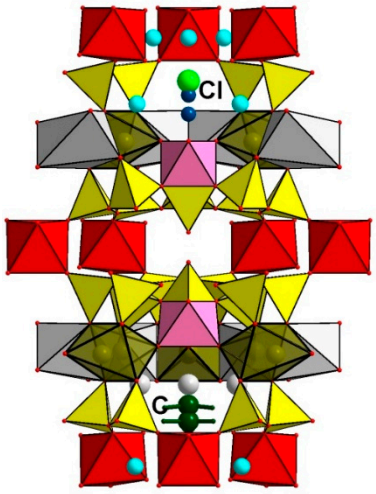

Figure 9. Blocky isomorphism in the *M*3 and *M*4 micro-regions of golyshevite viewed along (210).

Unlike Si-centered tetrahedra, the $NbO_3(OH)_3$ octahedra located in the *M*3 and *M*4 micro-regions can be directed towards the *N*5 cavity between the neighboring Si_9O_{27} rings only in the case when the *N*5 site is vacant. Otherwise this would result in unrealistic short distances between OH groups and *N*5 cations.

The option when the octahedra are oriented both outward and inward of the *N*5 cavity is extremely rare. This situation takes place in a low-silicon sample with high contents of niobium and titanium and a low content of zirconium, found in the Kovdor phlogopite deposit, Kola Peninsula (Figure 10). This centrosymmetric member of the eudialyte group was formed as the result of partial leaching of sodium from an earlier EGM [68]. In the micro-regions *M*3 and *M*4 of this mineral, there are two octahedral sites located at a distance of 2.19 Å from each other and populated by titanium with the occupancy factors of 50 and 30%, respectively. A TiO_6 octahedron with a population of 50% is directed inside the *N*5 cavity, while the less populated one faces in the opposite direction from the 9-membered ring. At a distance of 0.29 Å from the Ti site, there is a site occupied by Si with the population of 20%. Thus, all positions in the *M*3 and *M*4 micro-regions are populated statistically.

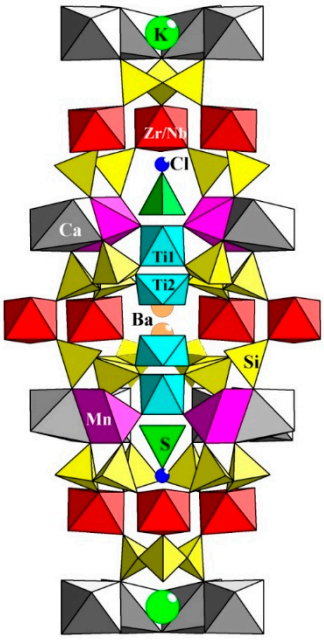

Figure 10. The crystal structute of a Nb,Ti-rich EGM from the Kovdor phlogopite deposit viewed along (210) [68].

4. Blocky Isomorphism at *N* Sites

At the *N*1–*N*5 extra-framework sites occurring in large cavities of the structures of EGMs, positional isomorphism of a statistical nature is most often observed. Below we will use the symbols *N*1–*N*5 to denote corresponding cavities (i.e., micro-regions containing several closely spaced extra-framework sites). In most cases, these positions are split and occupied by sodium; the set of closely spaced Na sites is typically coordinated by anions belonging to the same polyhedron. However, if significant amounts of other large cations enter these sites, ordering of different elements among closely spaced sites may result in changes in their anionic environment.

Most frequently, extra-framework cations other than Na occur at the *N*3 and *N*4 sites (Table 3). For example, in the structure of davinciite [52], the *N*3 and *N*4 cavities contain pairs of partially populated sites with the distances *N*3a–*N*3b = 0.65(1) Å and *N*4a–*N*4b = 0.42(1) Å. The *N*3a and *N*3b sites are partially occupied by K and (K + Na) and have 7- and 6-fold coordination, respectively. The 6-fold polyhedron is formed solely by O atoms of the framework, whereas the 7-fold polyhedron contains one H_2O molecule. The *N*4a and *N*4b sites are partially occupied by (Na + Sr) and Sr and have 8- and 7-fold coordination, respectively. The larger Sr-centered 8-fold polyhedron involves two Cl atoms, and smaller one contains only one Cl atom.

A remarkable example of blocky isomorphism at the *N* sites is presented in a Fe- and Na-deficient EGM [41,50,69]. In this sample, sodium deficiency of almost 50% compared to eudialyte *s.s.* is mainly compensated by hydronium groups H_3O^+, as well as subordinate K^+, Sr^{2+}, and Ce^{3+}. These cations occur in the *N*3 cavity and are statistically distributed over four sites, located at distances of 0.32(1) to 0.95(1) Å from each other. The coordination numbers and cation–anion distances (Å) for these sites are 10 and 2.91 for H_3O, 10 and 2.87 for K, 9 and 2.73 for Ce, and 7 and 2.61 for Sr.

In most samples of EGMs, including eudialyte, manganoeudialyte, kentbrooksite, ferrokentbrooksite, carbokentbrooksite, voronkovite, raslakite, sergevanite, and oneillite, the *N*3 and *N*4 sites are Na-dominant. However, in some members of the eudialyte group the *N*4 site is predominantly occupied by other cations: Sr (in taseqite), *REE* (in zirsilite-(Ce) and johnsenite-(Ce)), Mn (in georgbarsanovite and siudaite), and K (in andrianovite: Figure 8), etc.

Large *N*4-cations form triads of edge-sharing polyhedra. The coordination number of the *N*4 site in kentbrooksite, taseqite, and georgbarsanovite is equal to 10 (Figure 11) and is characterized by

the cation–anion distances from 2.471 to 2.943 Å. The *N*4 site in andrianovite has 8-fold coordination and the cation–anion distances from 2.557 to 2.980 Å. Mixed population is typical for the *N*4 site. For example, the composition of the *N*4 micro-region in georgbarsanovite and andrianovite is $(Mn_{1.07}Sr_{0.72}Ce_{0.47}Ca_{0.33}K_{0.25}Y_{0.16})_{\sum 3}$ and $(K_{1.45}Sr_{1.05}Ce_{0.5})_{\sum 3}$, respectively.

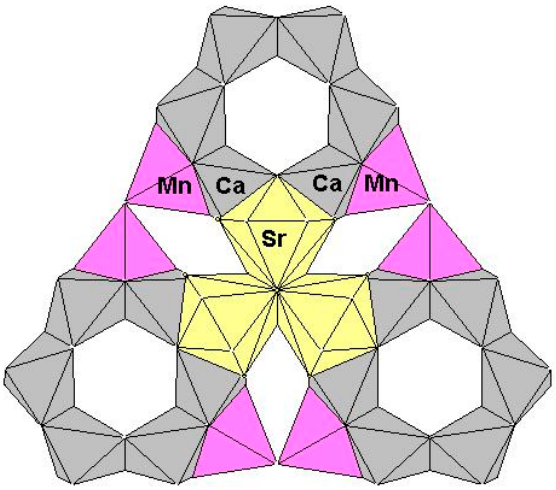

Figure 11. The layer formed by the $^{M1}Ca_6$, $^{N4}Sr_{10}$, and $^{N3}Mn^{2+}{}_5$ polyhedra in "eucolite" (Sr- and Mn-rich EGM viewed along (001) [27,34]).

In the majority of eudialyte-related minerals, the crystal chemical formula ($Z = 3$) contains 6 Ca atoms, which enter into the composition of the six-membered ring of octahedra, and the *N*3 and *N*4 sites are predominantly occupied by Na (Figure 12a). However, in specific environments, EGMs of a different stoichiometry are formed. In particular, there are three representatives of this group with a high content of calcium of 9 to 10 Ca *apfu*: feklichevite, golyshevite, and mogovidite (Table 1).

An example of EGM with an unusually high Ca content is feklichevite, $Na_{11}Ca_9Fe_2Zr_3NbSi_{25}O_{73}(OH,H_2O,O,Cl)_5$ [37]. In this mineral, Ca completely occupies the *M*1 site in the ring of octahedra and dominates at the neighboring *N*3 site. A cluster formed by three Ca-centered polyhedra sharing common vertices occurs at the threefold axis completed by six *M*1 octahedra (Figure 12b).

Golyshevite and mogovidite are the most Ca-rich EGMs (Table 3). In these minerals, Ca occupies the *M*1 site in the ring of octahedra and dominates over Na at *N*(4) (in golyshevite [39], Figure 12c) or at both *N*(3) and *N*(4) (in mogovidite [38]). In the latter case, a double layer of Ca-centered polyhedra is formed (Figure 12d).

The *N*3- and *N*4-centered polyhedra share common edges with the $M1O_6$ octahedra. As a result, the substitution of Na by bi- or trivalent cations at the *N*3 and *N*4 sites results in changes of local situations in the *M*2 micro-region and formation of rigid layers formed by the *M*1-, *M*2-, *N*3-, and *N*4-centered polyhedra. Acentric character of the georgbarsanovite crystal structure is especially obvious because of the presence of bi- and trivalent cations at the *N*4 site. As a result, this mineral demonstrates a pronounced piezo-effect.

The following local situations around the *M*2 micro-region are possible in Na-deficient EGMs:

1. $^{IV}M2 + {}^{VI}M1 + {}^{VI}M1 + {}^{VI–VIII}N3 + {}^{VI–VIII}N3$
2. $^{V}M2 + {}^{VI}M1 + {}^{VI}M1 + {}^{VI}M3 + {}^{VI–VIII}N3 + {}^{VI–VIII}N3$
3. $^{V}M2 + {}^{VI}M1 + {}^{VI}M1 + {}^{VI}M4 + {}^{VI–VIII}N3 + {}^{VI–VIII}N3$
4. $^{VI-VII}M2 + {}^{VI}M1 + {}^{VI}M1 + {}^{VI}M3 + {}^{VI}M4 + {}^{VI–VIII}N3 + {}^{VI–VIII}N3$
5. $^{IV}M2 + {}^{VI}M1 + {}^{VI}M1 + {}^{VI–VIII}N4 + {}^{VI–VIII}N4$
6. $^{V}M2 + {}^{VI}M1 + {}^{VI}M1 + {}^{VI}M3 + {}^{VI–VIII}N4 + {}^{VI–VIII}N4$
7. $^{V}M2 + {}^{VI}M1 + {}^{VI}M1 + {}^{VI}M4 + {}^{VI–VIII}N4 + {}^{VI–VIII}N4$
8. $^{VI-VII}M2 + {}^{VI}M1 + {}^{VI}M1 + {}^{VI}M3 + {}^{VI}M4 + {}^{VI–VIII}N4 + {}^{VI–VIII}N4$

9. $^{IV}M2 + {}^{VI}M1 + {}^{VI}M1 + {}^{VI–VIII}N3 + {}^{VI–VIII}N3 + {}^{VI–VIII}N4 + {}^{VI–VIII}N4$
10. $^{V}M2 + {}^{VI}M1 + {}^{VI}M1 + {}^{VI}M3 + {}^{VI–VIII}N3 + {}^{VI–VIII}N3 + {}^{VI–VIII}N4 + {}^{VI–VIII}N4$
11. $^{V}M2 + {}^{VI}M1 + {}^{VI}M1 + {}^{VI}M4 + {}^{VI–VIII}N3 + {}^{VI–VIII}N3 + {}^{VI–VIII}N4 + {}^{VI–VIII}N4$
12. $^{VI–VII}M2 + {}^{VI}M1 + {}^{VI}M1 + {}^{VI}M3 + {}^{VI}M4 + {}^{VI–VIII}N3 + {}^{VI–VIII}N3 + {}^{VI–VIII}N4 + {}^{VI–VIII}N4$

Table 3. Dominant components at the *N*3 and *N*4 sites of Na-depleted EGMs.

Mineral	*N*3	*N*4	Reference
Golyshevite	Na	Ca	[38,39]
Mogovidite	Ca	Ca	[38,64]
Feklichevite	Ca	Na	[37]
"Ferrofeklichevite"	Ca	Na	[70]
Taseqite	Na	Sr	[35,36]
Georgbarsanovite	Na	Mn	[33,34]
Zirsilite-(Ce)	Na	Ce	[71]
Johnsenite-(Ce)	Na	*REE*	[67]
Abdrianovite	Na	K, Sr	[30]
Davinciite	K	Na	[52]

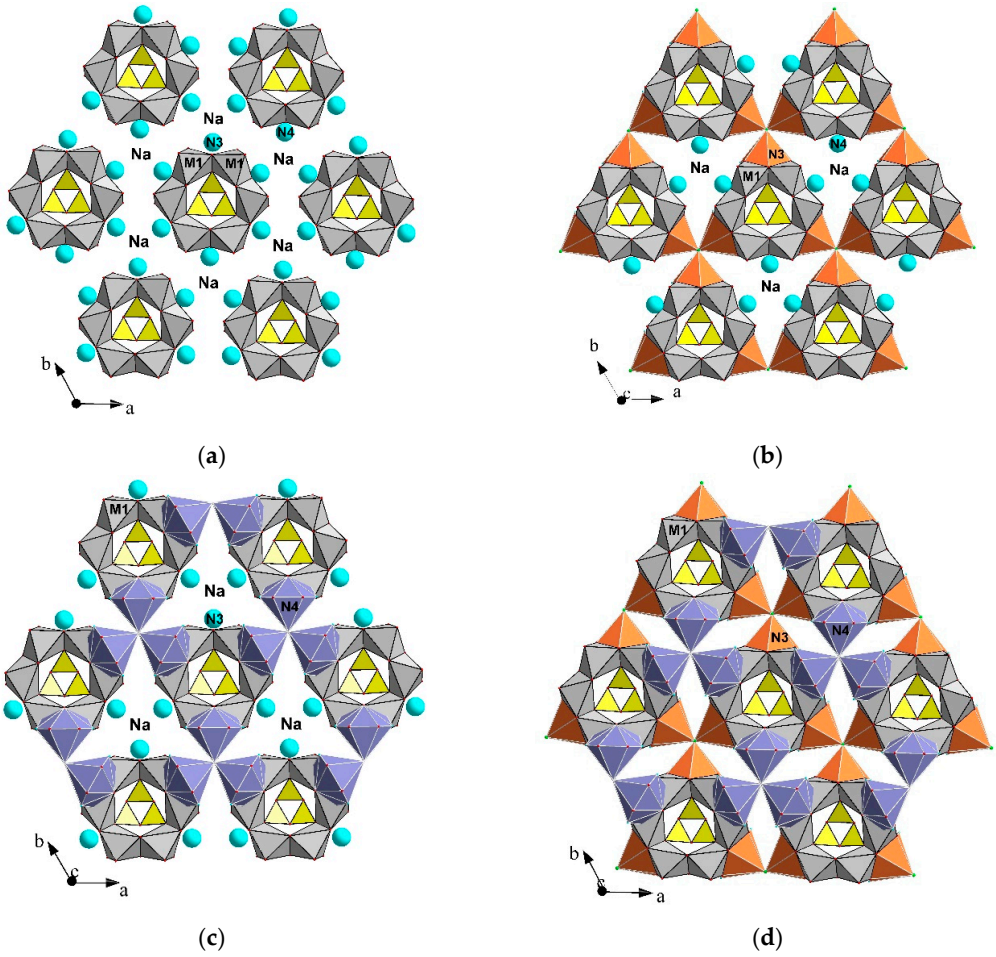

Figure 12. Layers consisting of ^{M1}Ca-, ^{N3}Na-, and ^{N4}Na-polyhedra in Na-rich EGMs (**a**); ^{M1}Ca-, ^{N3}Ca-, and ^{N4}Na-polyhedra in feklichevite (**b**); ^{M1}Ca-, ^{N3}Na-, and ^{N4}Ca-polyhedra in golyshevite (**c**); and ^{M1}Ca-, ^{N3}Ca-, and ^{N4}Ca-polyhedra in mogovidite (**d**).

5. Blocky Isomorphism at the *X* Sites

In the structures of EGMs, the extra-framework *X*1 and *X*2 sites located on the threefold axis can be occupied by different anions (Cl^-, F^-, S^{2-}, SO_4^{2-}, and CO_3^{2-}) and H_2O molecules which coordinate large *N* and (in some samples) *M*2 cations. The most common *X*-components are Cl^- (e.g., in eudialyte *s.s.*) and H_2O (e.g., in feklichevite). Carbonate anion is a significant component in five EGMs: golyshevite, mogovidite, carbokentbrooksite, johnsenite-(Ce), and zirsilite. The only EGM with species-defining F^- is kentbrooksite. S-bearing anions can occur at the *X* sites in subordinate amounts.

In zirsilite-(Ce) and carbokentbrooksite, the *X*1 site is split into two sub-sites, one of which is partly occupied by CO_3^{2-} and another one contains Cl^-. The total population of the *X*1 site is $C_{0.43}Cl_{0.3}$ in zirsilite-(Ce) and $C_{0.58}Cl_{0.27}$ in carbokentbrooksite. The *X*2 site in these minerals is occupied by H_2O.

In golyshevite, the *X*1 site is split into two sub-sites located at the distance of 0.55 Å from each other and occupied by CO_3^{2-} (with the total occupancy close to 100%), and the *X*2 site is occupied by H_2O and subordinate Cl^-. Both carbonate groups are flat triangles whose O atoms coordinate cations of the *N*4 micro-region (Figure 9).

In most S-bearing EGMs, sulfur occurs in the sulfate form. In these minerals, isolated SO_4 tetrahedra occur at the sites located on the threefold axis (see Figures 10 and 13). A potentially new EGM containing sulfur in the sulfide form has been discovered recently in the Lovozero alkaline massif, Kola Peninsula [72]. Hypothetically, this mineral crystallized at a low activity of oxygen. Its end-member formula is $(Na_{14}Sr)Ca_6(Mn_2Na)Zr_3[Si_{26}O_{72}](OH)_3S^{2-}\cdot 2H_2O$. In the sulfide EGM, the *X*1 and *X*2 sites are split into pairs of closely spaced sub-sites with the following occupancies: *X*1a = $0.41(S^{2-} + Cl)$, *X*1b = $0.39H_2O$, *X*2a = $0.33(S^{2-} + Cl)$, *X*2b = $0.30H_2O$. The S^{2-} anions belonging to the *X*1 and *X*2 micro-regions coordinate triads of Sr^{2+} and Na^+ cations with the Sr–S and Na–S distances of 2.322 and 2.541 Å, respectively.

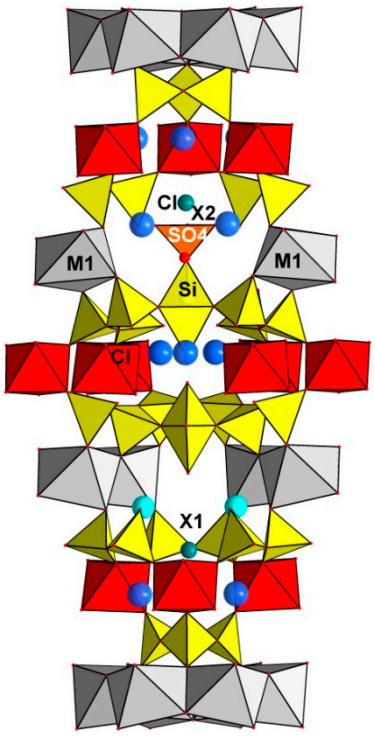

Figure 13. The crystal structure of aqualite viewed along (210).

6. Ordered Blocky Isomorphism in Modular EGMs

Heteropolyhedral frameworks of EGMs consist of layers containing Si_3O_9 and Si_9O_{27} rings of tetrahedra (*T*-layer), $^{VI}M1_6O_{24}$ rings of octahedra (*M*-layer), and isolated ZO_6 octahedra (*Z*-layer) alternating in the order (… *TMTZ* …). Most EGMs have 12-layer structures, with the 2D repeat unit $(TMTZ)_3$, unit-cell parameters $a \sim 14$ Å, $c \sim 30$ Å, and space groups $R\bar{3}m$, $R3m$, or $R3$. However, in several members of the eudialyte group (so-called "megaeudialytes"), additional cation ordering takes place which results in the formation of the doubled 2D repeat units $[(TMTZ)(T^*M^*T^*Z^*)]_3$ with the ordered 1:1 alternation of two nonequivalent *TMTZ* modules and doubling of the *c* parameter (c ~60–61 Å). Megaeudialytes are characterized by the same space groups as common 12-layer EGMs. Unlike crystalline compounds with superstructures, in megaeudialytes *R*-translation remains, and the unit-cell doubling is due to blocky isomorphism in the 30 Å module.

Megaeudialytes are known only in the Lovozero and Khibiny alkaline massifs, Kola Peninsula [1,4,73–79]. Four of them (alluaivite, dualite, labyrinthite, and rastsvetaevite) have been approved by the Commission on New Minerals, Nomenclature, and Classification of the IMA as valid mineral species (see Figures 14 and 15).

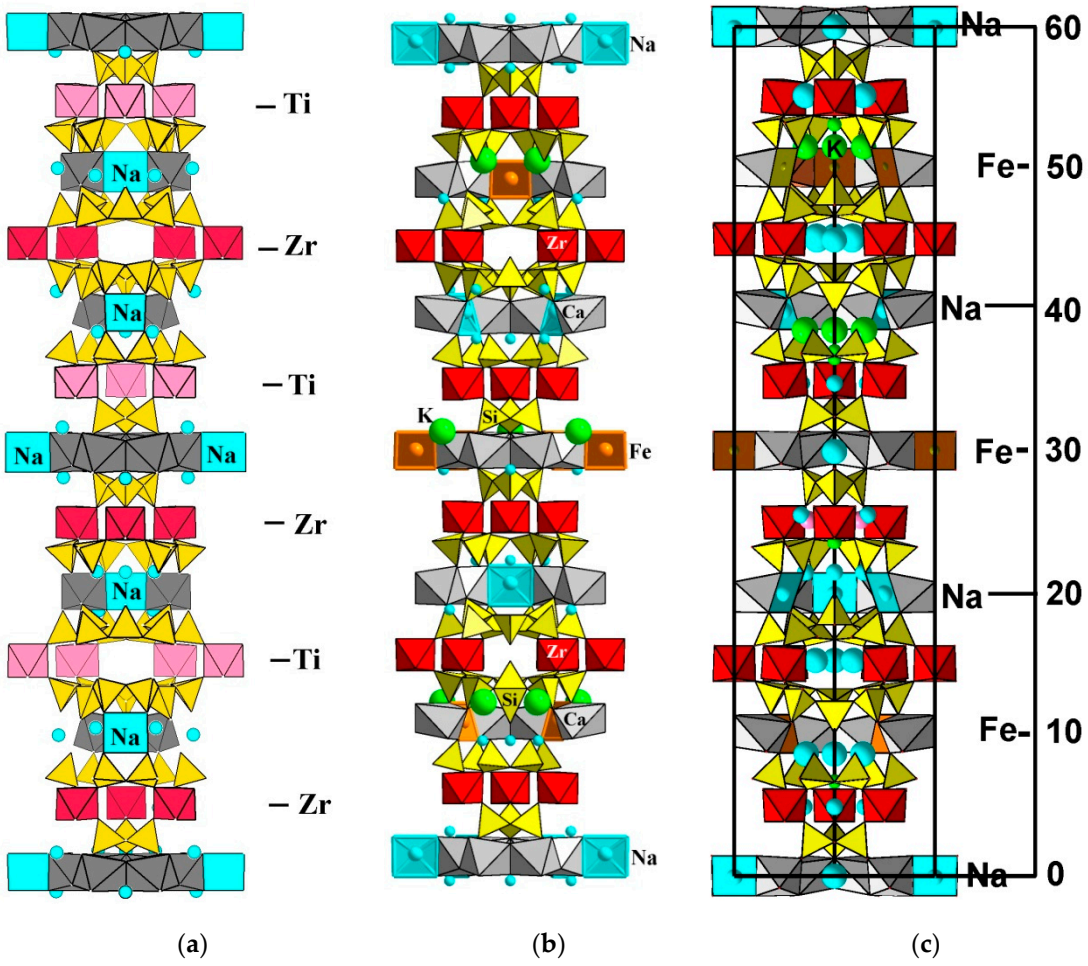

Figure 14. Ordered isomorphism at the *Z* site in dualite [73] (**a**), at the *M*2 and *N*3 sites in rastsvetaevite holotype [23,74] (**b**), and at the *M*2 and *N*4 sites in hydrated rastsvetaevite [8,75] (**c**), viewed along (210).

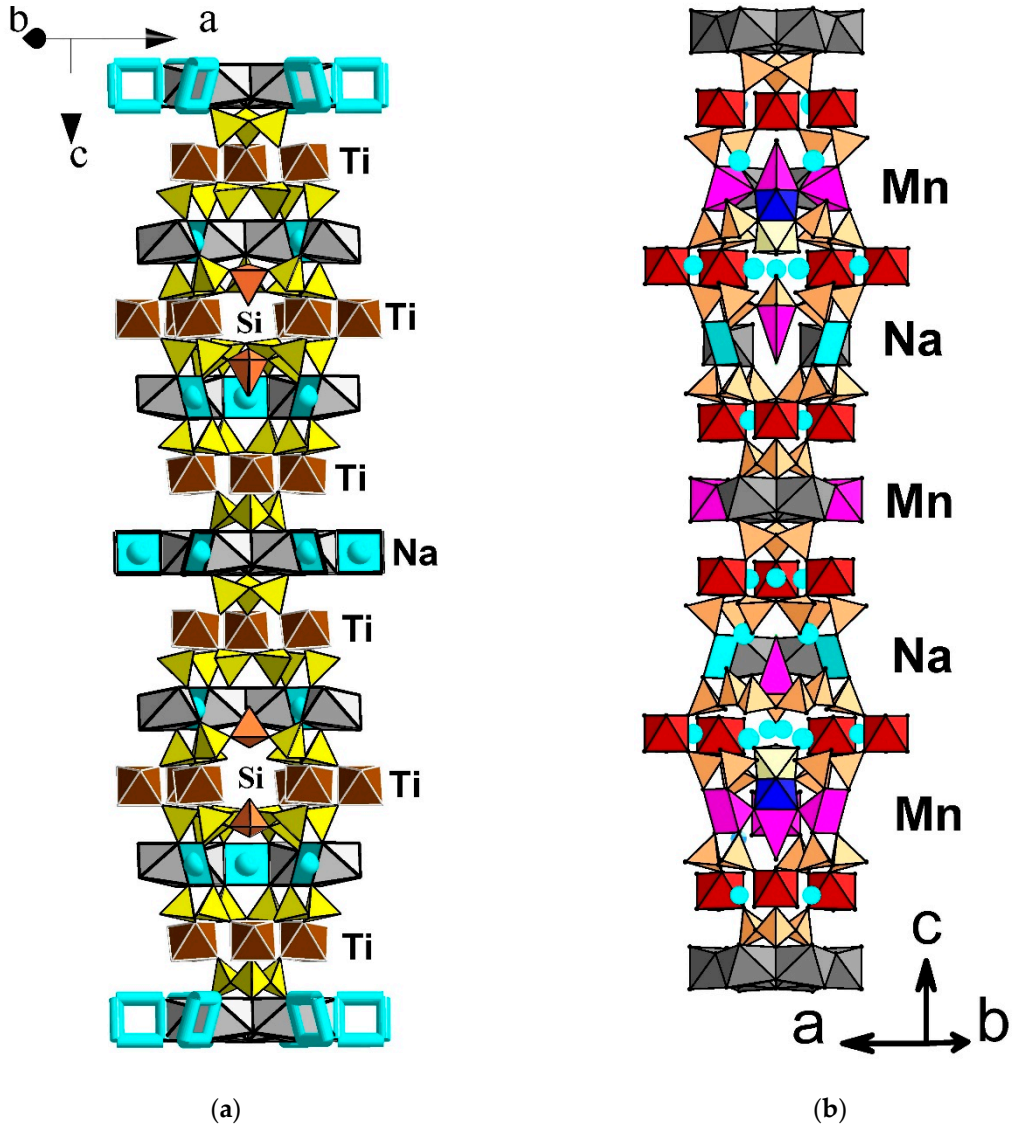

(**a**) (**b**)

Figure 15. The crystal structures of alluaivite (differently oriented SiO_4 tetrahedra at the *M*3 and *M*4 sites are shown with red) (**a**) and Mn-rich "megaeudialyte" with the alteration of $^{M2}(^{IV}Na)$ and $^{M2}(^{V}Mn^{2+})$ in neighboring modules [24] (**b**).

Unlike zirconium, titanium rarely forms isolated octahedra in structures of silicate minerals [80]. The main cause of this distinction between the behavior of these elements is a different degree of distortion of Zr- and Ti-centered octahedra. As a result, the isomorphism between Ti and Zr is usually significantly restricted. Minerals of the eudialyte group are one of exceptions to this rule. In EGMs, titanium can occur at the *M*2, *M*3, and *M*4 sites (Table 4).

Table 4. Ordered blocky isomorphism at the *M*2 and *M*3/*M*4 sites of EGMs with modular structures and doubled *c* parameter (*Z* = 3).

No.	Mineral	Module I		Module II		References
		*M*3+*M*4	*M*2	*M*3*+*M*4*	*M*2*	
1	Alluaivite holotype (*Z* = Ti)	Si_2 ↑	$^{VII}Na_{2.34}$ $^{IV}Na_{0.66}$	Si_2 ↓	$^{IV}Na_3$	[81]
2	Alluaivite (*Z* = Ti)	Si_2 ↑	$^{IV}Na_{1.6}{}^{V}Mn_{1.4}$	Si_2 ↓	$^{IV}Na_3$	[18]
3	Dualite holotype ($Z = Z_{Zr} + Z_{Ti}$)	$^{IV}Mn_{1.64}$ $Si_{0.36}$	$^{V}Na_{1.3}{}^{VI}Ti_{1.0}$ $^{IV}Fe_{0.7}$	Si_2	$^{V}Na_{1.7}{}^{V}Mn_1$ $^{IV}Fe_{0.3}$	[43,73]
4	Rastsvetaevite holotype	$Si_{1.5}{}^{VI}Al_{0.2}$ $^{VI}Nb_{0.1}$	$^{VII}K_2{}^{VII}K_2$ $^{IV}Na_{1.0}$	Si_2	$^{IV}Fe_{1.9}{}^{V}Na_{0.5}$ $^{V}Mn_{0.3}{}^{V}Fe_{0.3}$	[74,78]
5	Labyrinthite holotype	$Si_{1.2}{}^{VI}Ti_{0.5}$	$^{IV}Fe_{2.2}Mn^{V}{}_{0.8}$	Si_2	$^{IV}Na_{1.2}{}^{VII}Na_{1.7}$ $^{VII}Na_{1.6}$	[23,77]
6	K-deficient rastsvetaevite	Si_2	$^{VII}K_{4.6}{}^{IV}Na_{0.5}$	Si_2	$^{IV}Fe_{2.2}$ $^{V}Mn_{0.5}{}^{V}Fe_{0.3}$	[8]
7	"Hyper-Mn EGM"	Si_2	$^{V}Mn_{2.46}{}^{V}Fe_{0.18}$ $^{VI}Na_{1.86}$	Si_2	$^{IV}Na_{2.4}{}^{VI}Na_{1.2}$	[24]
8	Labyrinthite $R\bar{3}m$ analogue	$Si_{1.3}{}^{VI}Ti_{0.5}$ $^{VI}Nb_{0.1}$	$^{IV}Fe_{1.0}$ $^{V}K_{1.5}{}^{V}Sr_{0.5}$	Si_2	$^{V}Mn_{1.6}{}^{IV}Fe_{0.9}$	[79]
9	Hydrated rastsvetaevite	$Si_{1.4}{}^{VI}Nb_{0.2}$	$^{IV}Na_{1.0}{}^{IV}Sr_{0.6}$	$Si_{1.4}{}^{VI}Ti_{0.2}$	$^{IV}Fe_{2.2}{}^{V}Mn_{0.6}$	[8]
10	Hydrated rastsvetaevite	Si_2	$^{IV}Na_{2.7}{}^{V}Fe_{0.3}$	$Si_{1.7}{}^{VI}Ti_{0.3}$	$^{V}Fe_{2.0}{}^{V}Mn_{0.8}$	[75]
11	Centrosymmetric EGM	Si_2	$^{IV}Fe_{1.23}$	Si_2	$^{IV}Na_{2.01}{}^{V}Mn_{0.63}$ $^{VI}Sr_{0.6}$	[76]

Note: Orientation of Si-centered tetrahedra at the *M*3 and *M*4 sites of alluaivite is shown with arrows.

Alluaivite (Sample 1 in Table 4; Figure 15) [81] is the first megaeudialyte whose crystal structure was solved. In this mineral zirconium is absent, and the *Z* and *Z** sites are occupied by Ti and subordinate Nb. The substitution of Zr^{4+} by the smaller cation Ti^{4+} results in the lowering of unit-cell parameters (by 0.1–0.2 Å for *a* and 0.1–0.3 Å for *c*). Both the *M*2 and *M*2* micro-regions (in the modules I and II, respectively) are occupied by Na. All Na in the *M*1 micro-region has fourfold flat-square coordination. In the *M*2 micro-region, Na is distributed among three sites: one site having flat-square coordination and two sites with 7-fold coordination located on both sides from the square. Another cause of the unit-cell doubling is blocky isomorphism in the *M*3 and *M*4 micro-regions; in each module, both additional SiO_4 tetrahedra have the same orientation, but their orientation is different in different modules.

In the structure of dualite (Sample 3 in Table 4; see Figure 14a) [43], alternation of Zr and Ti in the modules I and II takes place. The *M*3 + *M*4 and *M*3* + *M*4* micro-regions of dualite are dominated by ^{IV}Mn and Si, respectively. There are also significant differences in the populations of the ^{V}Na-dominant *M*2 and *M*2* sites of dualite.

The unit-cell doubling of rastsvetaevite (Sample 4 in Table 4; see Figure 14b) [78] is mainly due to the blocky isomorphism in the *M*2 and *M*2* micro-regions: in *M*2, Na has fourfold flat-square coordination and is surrounded by K atoms having sevenfold coordination; the micro-region *M*2* is predominantly occupied by Fe. There are also differences between the modules I and II of rastsvetaevite in the population of extra-framework sites. In particular, in the module I the *N*3 site is occupied by K, whereas in the module II all *N* sites are Na-dominant.

In most cases, the formation of megaeudialytes is regulated by the ordering of the *M*2-cations. For example, in hydrated rastsvetaevite (Sample 10 in Table 4; see Figure 14c) [75], different population of the *M*2 and *M*2* micro-regions (by $^{IV}Na_{2.7}{}^{V}Fe_{0.3}$ and $^{V}Fe_{2.0}{}^{V}Mn_{0.8}$, respectively) is the main cause of the unit-cell doubling.

7. Combinations of Blocky Isomorphism at the *M*1–*M*4 Sites

The population of each of the *M*1–*M*4 micro-regions does not occur independently on the local situations at neighboring sites. Very often, *M*2-centered polyhedra share common edges with the $M1O_6$ octahedra and common vertices with the $M3O_6$ and $M4O_6$ octahedra. As a result, only specific kinds of clusters (i.e., combinations of local situations around neighboring *M*1–*M*4 cations) can be realized with their statistical alteration in different unit cells. The examples of different clusters which can be involved in the combined blocky isomorphism in EGMs with the symmetry *R*3*m* (1–4) and *R*3 (5–8) are

1. $^{IV}M2 + {}^{VI}M1 + {}^{VI}M1$
2. $^{V}M2 + {}^{VI}M1 + {}^{VI}M1 + {}^{VI}M3$
3. $^{V}M2 + {}^{VI}M1 + {}^{VI}M1 + {}^{VI}M4$
4. $^{VI\text{-}VII}M2 + {}^{VI}M1 + {}^{VI}M1 + {}^{VI}M3 + {}^{VI}M4$
5. $^{IV}M2 + {}^{VI}M1.1 + {}^{VI}M1.2$
6. $^{V}M2 + {}^{VI}M1.1 + {}^{VI}M1.2 + {}^{VI}M3$
7. $^{V}M2 + {}^{VI}M1.1 + {}^{VI}M1.2 + {}^{VI}M4$
8. $^{VI\text{-}VII}M2 + {}^{VI}M1.1 + {}^{VI}M1.2 + {}^{VI}M3 + {}^{VI}M4$

The $M1O_6$ octahedra can be occupied by different elements including Ca, Mn, Fe, Na, *REE*, Sr, and Y. For example, in one module of dualite, all the listed elements, except Y statistically substitute each other [43]. For each cluster involving the *M*1 and *M*2 polyhedra, only specific combinations of cations which answer the condition of local valence balance on the common O atom are possible. Some examples are presented in Figures 16 and 17.

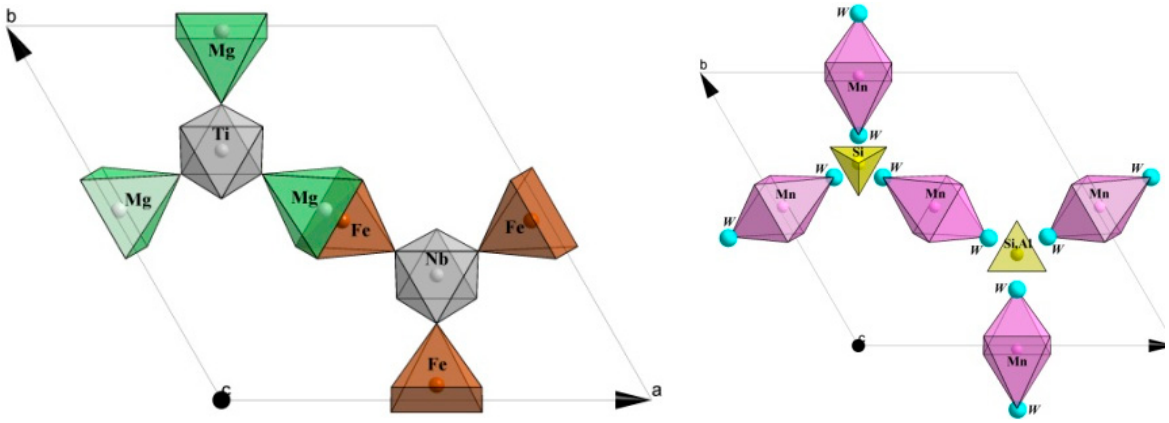

(**a**) (**b**)

Figure 16. Alternative variants of blocky isomorphism in the structure of manganoeudialyte [58], with the *M*2 micro-region occupied by differently oriented Mg- and Fe-centered square pyramids (**a**) and by Mn-centered octahedra (**b**) viewed along (001).

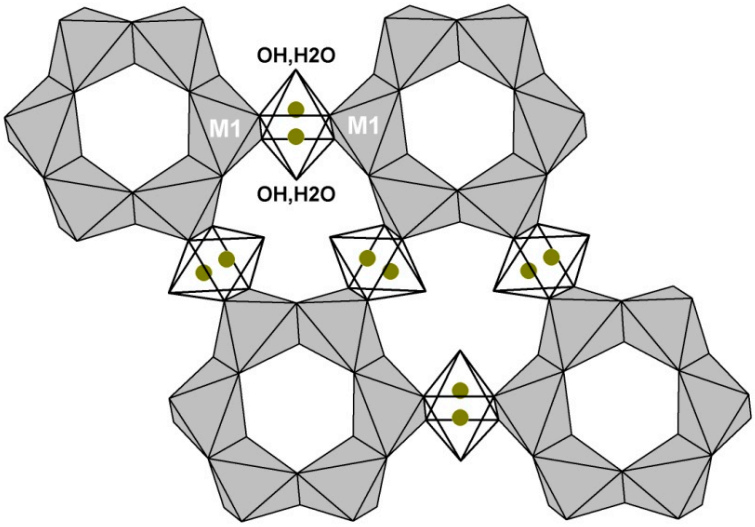

Figure 17. Pairs of differently oriented $M2O_5$ pyramids in the structure of a ^{V}Na-dominant sample viewed along (001) [15].

In kentbrooksite, barsanovite and some related EGMs, the $^{M2}Mn^{2+}O_5$ and $^{M2}Fe^{2+}O_5$ polyhedra are combined with the $^{M3,M4}Nb^{5+}O_6$ octahedra. In W-dominant EGMs related to kentbrooksite (i.e., khomyakovite, manganokhomyakovite, and johnsenite-(Ce)), the $^{M2}Mn^{2+}O_5$ and $^{M2}Fe^{2+}O_5$ pyramids are combined with the $^{M3,M4}W^{6+}O_6$ octahedra. In these cases, local charge balance is regulated by the isomorphism between O and OH at the common vertex of the square pyramid and octahedron.

The charge of *M*2-cations, which occur in different polyhedra having common edges with the $M1O_6$ octahedra, can vary from 1 to 5, but cations with high charges (Ti^{4+}, Zr^{4+}, and Ta^{6+}) cannot occupy the *M*2 micro-region in combination with trivalent *M*1 cations (Ln^{3+}, Y^{3+}). In high-calcium EGMs like mogovidite, feklichevite, golyshevite, and ferrofeklichevite, the *M*2 micro-region can contain bi-, tri-, tetra-, and pentavalent cations. In other cases, different combinations of uni-, bi-, and trivalent *M*1-cations with *M*2-cations having charges from +1 to +5 are realized.

A high degree of separation of different elements in the *M*2 micro-region is realized in a Fe-deficient sample from the Oleniy Ruchey deposit, Khibiny massif, Kola Peninsula [10]. Its crystal-chemical formula is ($Z = 3$):

$^{N1–5}[(Na_{11.1}(H_3O)_{2.4}Ln_{0.3}]\,^{N6}[K_{0.5}]\,^{M1}[Ca_{4.9}(Mn_{1.1})]\,^{\boldsymbol{M2}}\boldsymbol{[^{IV}Fe_{0.9}\,^{VI}Na_{0.7}\,^{V}Na_{0.6}\,^{VII}Mn_{0.5}\,^{V}(Mn,Fe)_{0.3}]}$ $^{M3,M4}[Si_{1.8}Nb_{0.2}]\;^{Z}[Zr_{2.6}Ti_{0.4}]\;[Si_{24}O_{72}]\;[SO_4]_{0.25}(OH)_{2.4}Cl_{0.5}(H_2O,OH)\cdot 1.5H_2O$. In this mineral, four kinds of clusters (1 to 4 types) involving five kinds of *M*2-polyhedra are realized statistically.

A more complex situation takes place in Ca-depleted samples, in which ordering in the *M*2 micro-region is accompanied by the ordering in the *M*1 sites of the 6-membered ring of octahedra. In this case, the *M*1 site is transformed into two alternating sites, *M*1.1 and *M*1.2 (Figure 18), which are occupied differently (respectively, by Ca and Mn in oneillite and sergevanite, by Ca and Fe in raslakite, and by Mn and Na in voronkovite). Differently occupied octahedra have different sizes (Table 5) which results in variations of configurations of *M*2-polyhedra.

Table 5. Cation–oxygen distances (Å) in the *M*1a- and *M*1b-octahedra of ordered EGMs with the *R*3 symmetry.

No.	Mineral	Dominant Cations				References
		Ca	Mn	Fe	Na	
1	Oneillite	(2.431)	(2.227)			[82]
2	Raslakite	2.311–2.400 (2.362)		2.225–2.351 (2.306)		[57]
3	Voronkovite		2.132–2.278 (2.22)		2.393–2.497 (2.45)	[83,84]
4	Sergevanite	2.331–2.438 (2.381)	2.257–2.384 (2.309)			[85]
5	Sergevanite	2.320–2.420 (2.38)	2.230–2.386 (2.303)			[20]
6	Ca-deficient EGM	2.300–2.441 (2.37)	2.23–2.33 (2.29)			[86]
7	Ca-deficient EGM	2.27–2.411 (2.36)	2.211–2.38 (2.29)			[86]
8	Zr-rich EGM	2.30–2.41 (2.35)		2.228–2.347 (2.285)		[56,87]
9	Zr-rich EGM	2.297–2.38 (2.35)	2.211–2.38 (2.29)			[88]
10 *	Hydrated EGM	2.28–2.50 (2.37)			2.23–2.41 (2.34)	[89]

Note: Mean *M*1,2–O distances are given in brackets. The table includes holotypes of oneillite (1), raslakite (2), voronkovite (3), and sergevanite (4). * Megaeudialyte with c = 60.33 Å.

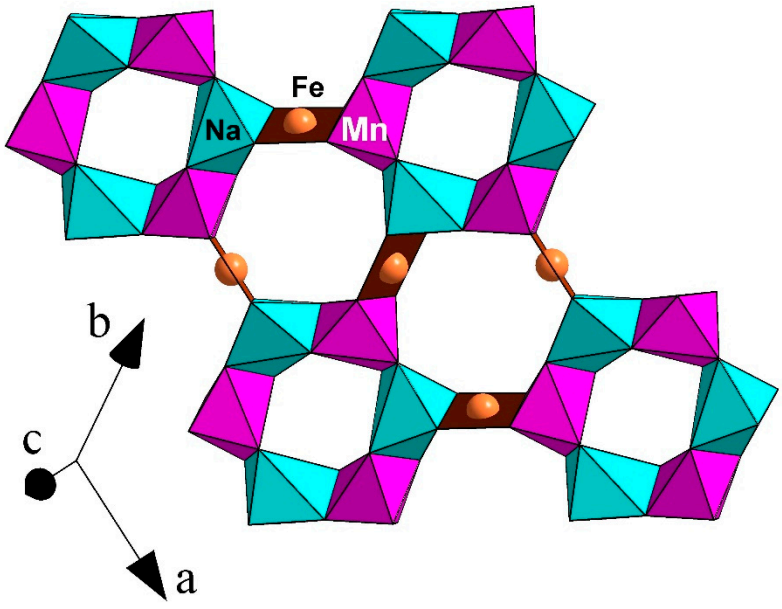

Figure 18. A fragment of the crystal structure of voronkovite [83].

8. Conclusions

The uniqueness of the eudialyte-group minerals lies in the combination of complexity and variability of their crystalline structures and various schemes of homovalent, heterovalent, and blocky isomorphism, in which at least 26 different elements are involved. From the crystal chemical point of view, the most interesting are the complex mechanisms of blocky isomorphism, when, in a given

micro-region of a unit cell, the substitution of one group of atoms and ions by another one is accompanied by significant changes of the local structure, including splitting of cationic and anionic sites, changes in the valence state and coordination numbers of cations. Such substitution schemes are realized both around the key sites of rigid high-force-strength cations of the framework (*M*2, *M*3, and *M*4), and in the *N*1–5 and *X*1–2 micro-regions, populated by extra-framework cations and anions, respectively.

Author Contributions: R.K.R. and N.V.C. analyzed literature data on the crystal chemistry of the eudialyte-group minerals and wrote the review. All authors have read and agreed to the published version of the manuscript.

Funding: This work was supported by the Ministry of Science and Higher Education within the State assignment FSRC «Crystallography and Photonics» RAS and state task, state registration number AAAA-A19-119092390076-7 (search and analysis of published data on EGMs), and the Russian Science Foundation, projects nos. 18-29-12005 (X-ray crystal structure analysis) and 18-29-12007-mk (crystal-chemical analysis).

Conflicts of Interest: The authors declare no conflict of interest.

References

1. Rastsvetaeva, R.K.; Chukanov, N.V.; Aksenov, S.M. *Minerals of Eudialyte Group: Crystal Chemistry, Properties, Genesis*; University of Nizhniy Novgorod: Nizhniy Novgorod, Russia, 2012; p. 230. ISBN 978-5-91326-207-3. (In Russian)
2. Johnsen, O.; Grice, J.D.; Gault, R.A. The crystal chemistry of the eudialyte group. *Canad. Mineral.* **1999**, *37*, 865–891.
3. Johnsen, O.; Ferraris, G.; Gault, R.A.; Grice, J.D.; Kampf, A.R.; Pekov, I.V. The nomenclature of eudialyte group minerals. *Canad. Mineral.* **2003**, *41*, 785–794. [CrossRef]
4. Rastsvetaeva, R.K.; Khomyakov, A.P. Crystal chemistry of modular eudialytes. *Cryst. Rep.* **2003**, *48*, S78–S90.
5. Rastsvetaeva, R.K. Structure mineralogy of eudialyte group. *Cryst. Rep.* **2007**, *52*, 47–64. [CrossRef]
6. Rastsvetaeva, R.K.; Chukanov, N.V. Classification of eudialyte-group minerals. *Geol. Ore Depos.* **2012**, *54*, 487–497. [CrossRef]
7. Rastsvetaeva, R.K.; Chukanov, N.V.; Aksenov, S.M. Crystalchemical principles of classifying the Eudialyte group. In Proceedings of the 35th International Geological Congress, Cape Town, South Africa, 27 August–4 September 2016; p. 4193.
8. Rastsvetaeva, R.K.; Aksenov, S.M.; Rozenberg, K.A. Crystal structure and genesis of hydrated analog of rastsvetaevite. *Cryst. Rep.* **2015**, *60*, 897–905. [CrossRef]
9. Khomyakov, A.P. *Mineralogy of Ultra-Agpaitic Alkaline Rocks*; Nauka: Moscow, Russia, 1990; p. 196.
10. Rastsvetaeva, R.K.; Chukanov, N.V.; Lisitsin, D.V. New data on the isomorphism in eudialyte-group minerals. IX. Blocky isomorphism in key sites. Crystal structure of a Fe-deficient eudialyte from the Khibiny Massif. *Cryst. Rep.* **2021**, *66*. in press.
11. Rastsvetaeva, R.K.; Chukanov, N.V. New data on the isomorphism in eudialyte-group minerals. X. Crystal structure of an intermediate member of the raslakite–sergevanite solid-solution series. *Cryst. Rep.* **2021**, *66*. in press.
12. Rastsvetaeva, R.K.; Aksenov, S.M.; Chukanov, N.V. New data on crystal chemistry of eudialyte-group minerals. In Proceedings of the XIX International Meeting on Crystal Chemistry, X-ray Diffraction and Spectroscopy of Minerals, Apatity, Russia, 2–8 July 2019; p. 81.
13. Rastsvetaeva, R.K.; Aksenov, S.M.; Chukanov, N.V. New data on the crystal chemistry and systematics of minerals of eudialyte group. *Cryst. Probl.* **2019**, *7*, 192–202. (In Russian)
14. Solodovnikov, S.F. *Main Terms and Conceptions of Structural Crystallography and Crystal Chemistry*; Institute of Inorganic Chemistry: Novosibirsk, Russia, 2005; p. 114.
15. Rastsvetaeva, R.K.; Chukanov, N.V.; Pekov, I.V.; Schäfer, C.; Van, K.V. New data on the isomorphism in eudialyte-group minerals. 1. Crystal chemistry of eudialyte-group members with Na incorporated into the framework as a marker of hyperagpaitic conditions. *Minerals* **2020**, *10*, 587. [CrossRef]
16. Golyshev, V.M.; Simonov, B.I.; Belov, N.B. On the crystal structure of eudialyte. *Kristallografiya* **1971**, *16*, 93–98.
17. Golyshev, V.M.; Simonov, B.I.; Belov, N.B. The crystal structure of eudialyte. *Kristallografiya* **1972**, *17*, 1119–1123. (In Russian)

18. Rastsvetaeva, R.K.; Viktorova, K.A.; Aksenov, S.M. New data on the isomorphism in eudialyte-group minerals. IV. Modular structure of titanosilicate with replacement of Na by Mn in the alluaivite module. *Cryst. Rep.* **2019**, *64*, 586–589. [CrossRef]
19. Rozenberg, K.A.; Rastsvetaeva, R.K.; Khomyakov, A.P. Decationized and hydrated eudialytes. Oxonium problem. *Eur. J. Miner.* **2005**, *17*, 875–882. [CrossRef]
20. Rastsvetaeva, R.K.; Aksenov, S.M.; Chukanov, N.V. Crystal structure of the Mn analogue of raslakite, a new representative of the eudialyte group. *Dokl. Chem.* **2010**, *431*, 76–81. [CrossRef]
21. Rastsvetaeva, R.K.; Khomyakov, A.P. Crystal structure features of Na,Fe-decationized eudialyte with *R*3 symmetry. *Cryst. Rep.* **2002**, *47*, 232–236. [CrossRef]
22. Rastsvetaeva, R.K.; Khomyakov, A.P.; Andrianov, V.I.; Gusev, A.I. Crystal structure of alluaivite. *Dokl. Akad. Nauk. SSSR* **1990**, *312*, 1379–1383. (In Russian)
23. Rastsvetaeva, R.K.; Khomyakov, A.P. Modular structure of high sodium eudialyte analog with doubled *c*-period and *R*3 symmetry. *Cryst. Rep.* **2001**, *46*, 827–832.
24. Rastsvetaeva, R.K.; Ivanova, A.G.; Khomyakov, A.P. Modular structure of hypermanganese eudialyte. *Doklady Earth Sci.* **2006**, *410*, 1075–1079. [CrossRef]
25. Rastsvetaeva, R.K.; Khomyakov, A.P. Crystal structure of hyperzirconium analog of eudialyte. *Cryst. Rep.* **2000**, *45*, 219–221. [CrossRef]
26. Rastsvetaeva, R.K.; Chukanov, N.V.; Möckel, S. Characteristic structural features of a tantalum-rich eudialyte variety from Brazil. *Cryst. Rep.* **2003**, *48*, 216–221. [CrossRef]
27. Rastsvetaeva, R.K.; Razmanova, Z.P.; Borutsky, B.E.; Dorfman, M.D. Specific features of the crystal structure of barsanovite, a variety of eudialyte. *Proc. Sov. Mineral. Soc.* **1990**, *119*, 65–73. (In Russian)
28. Rozenberg, K.A.; Rastsvetaeva, R.K.; Verin, I.A. Crystal structure of centrosymmetrical 12-layer high sodium eudialyte. *Cryst. Rep.* **2009**, *54*, 446–450. [CrossRef]
29. Johnsen, O.; Grice, J.D.; Gault, A. Kentbrooksite from the Kangerdlugssuaq intrusion, East Greenland, a new Mn-*REE*-Nb-F end-member in a series within the eudialyte group: Description and crystal structure. *Eur. J. Mineral.* **1998**, *10*, 207–219. [CrossRef]
30. Rastsvetaeva, R.K.; Khomyakov, A.P. Crystal structure of a K analogue of kentbrooksite. *Doklady Chem.* **2005**, *403*, 148–151. [CrossRef]
31. Khomyakov, A.P.; Nechelyustov, G.N.; Rastsvetaeva, R.K.; Rozenberg, K.A. Andrianovite, $Na_{12}(K,Sr,Ce)_3Ca_6Mn_3Zr_3Nb(Si_{25}O_{73})(O,H_2O,OH)_5$, a new potassium-rich mineral species of the eudialyte group from the Khibiny alkaline Pluton, Kola Peninsula, Russia. *Geol. Ore Depos.* **2008**, *50*, 705–712. [CrossRef]
32. Johnsen, O.; Gault, R.A.; Grice, J.D. Ferrokentbrooksite, a new member of the eudialyte group from Mont Saint-Hilaire, Quebec. *Canad. Mineral.* **2003**, *41*, 55–60. [CrossRef]
33. Khomyakov, A.P.; Nechelyustov, G.N.; Ekimenkova, I.A.; Rastsvetaeva, R.K. Georgbarsanovite, $Na_{12}(Mn,Sr,REE)_3Ca_6Fe_3^{2+}Zr_3NbSi_{25}O_{76}Cl_2{\cdot}H_2O$, a mineral species of the eudialyte group: Revalidation of barsanovite and the new name of the mineral. *Zapiski Rossiiskogo Mineral. Obshchestva (Proc. Rus. Mineral. Soc.)* **2005**, *134*, 47–57. (In Russian)
34. Ekimenkova, I.A.; Rastsvetaeva, R.K.; Khomyakov, A.P. Crystal structure of the Fe,Cl-analogue of kentbrooksite. *Doklady Chem.* **2000**, *370*, 17–20.
35. Ekimenkova, I.A.; Rastsvetaeva, R.K.; Khomyakov, A.P. Refinement of the crystal structure of a Fe,Sr-analogue of kentbrooksite. *Kristallografiya* **2000**, *45*, 1010–1013. (In Russian) [CrossRef]
36. Petersen, O.V.; Johnsen, O.; Gault, R.A.; Niederayr, G.; Grice, A.D. Taseqite, a new member of the eudialyte group from the Ilímaussaq alkaline complex, South Greenland. *Neues Jahrb. Mineral.-Monatshefte* **2004**, *2*, 83–96. [CrossRef]
37. Rastsvetaeva, R.K.; Ekimenkova, I.A.; Pekov, I.V. Crystal structure of a new Ca-rich analogue of eudialyte. *Doklady Akademii Nauk.* **1999**, *368*, 636–638. (In Russian)
38. Chukanov, N.V.; Moiseev, M.M.; Rastsvetaeva, R.K.; Rozenberg, K.A.; Zadov, A.E.; Pekov, I.V.; Korovushkin, V.V. Golyshevite $(Na,Ca)_{10}Ca_9Fe_2Zr_3NbSi_{25}O_{72}(OH)_3(CO_3){\cdot}H_2O$ and mogovidite $Na_9(Ca,Na)_6Ca_6Fe_2Zr_3\square Si_{25}O_{72}(CO_3)(OH,H_2O)_4$—New eudialyte-group minerals from hypercalcium pegmatites of Kovdor. *Zapiski Rossiiskogo Mineral. Obshchestva (Proc. Russ. Mineral. Soc.)* **2005**, *134*, 36–47. (In Russian)

39. Rozenberg, K.A.; Rastsvetaeva, R.K.; Chukanov, N.V.; Verin, I.A. Crystal structure of golyshevite. *Cryst. Rep.* **2005**, *50*, 539–543. [CrossRef]
40. Rastsvetaeva, R.K.; Borutskiy, B.E.; Gusev, A.I. The crystal structure of eucolite. *Kristallografiya* **1988**, *33*, 353. (In Russian)
41. Rastsvetaeva, R.K.; Khomyakov, A.P. The crystal structure of the low-iron analogue of eudialyte. *Dokl. Akad. Nauk* **1998**, *362*, 784–788. (In Russian)
42. Ekimenkova, I.A.; Rastsvetaeva, R.K.; Chukanov, N.V. Ordering of calcium and iron in a mineral of the eudialyte group with the symmetry *R*3. *Dokl. Chem.* **2000**, *374*, 195–198.
43. Rastsvetaeva, R.K.; Khomyakov, A.P.; Chapuis, G. Crystal structure and crystal-chemical features of a new Ti-rich member of the eudialyte family. *Z. Krist.* **1999**, *214*, 271–278. [CrossRef]
44. Rastsvetaeva, R.K.; Khomyakov, A.P. Crystal structure of a new eudialyte analog with the *R*3 symmetry. *Cryst. Rep.* **1999**, *44*, 765–769.
45. Rastsvetaeva, R.K.; Chukanov, N.V.; Möckel, S.; Dudka, A.P.; Aksenov, S.M. New data on the isomorphism in eudialyte-group minerals. V: Crystal structure of an intermediate member of the manganoeudialyte-ilyukhinite isomorphous Series. *Cryst. Rep.* **2020**, *65*, 32–37. [CrossRef]
46. Rastsvetaeva, R.K.; Chukanov, N.V.; Van, K.V. New Data on the isomorphism in eudialyte-group minerals. VII. Crystal structure of the eudialyte—Sergevanite mineral series from the Lovozero alkaline massif. *Cryst. Rep.* **2020**, *65*, 555–561. [CrossRef]
47. Rastsvetaeva, R.K.; Rozenberg, K.A.; Chukanov, N.V.; Aksenov, S.M. Crystal structure of ilyukhinite, a new mineral of the eudialyte group. *Cryst. Rep.* **2017**, *62*, 60–65. [CrossRef]
48. Chukanov, N.V.; Rastsvetaeva, R.K.; Rozenberg, K.A.; Aksenov, S.M.; Pekov, I.V.; Belakovsky, D.I.; Kristiansen, R.; Van, K.V. Ilyukhinite, $(H_3O,Na)_{14}Ca_6Mn_2Zr_3Si_{26}O_{72}(OH)_2{\cdot}3H_2O$, a new mineral of the eudialyte group. *Geol. Ore Depos.* **2017**, *59*, 592–600. [CrossRef]
49. Chukanov, N.V.; Rastsvetaeva, R.K.; Kruszewski, Ł.; Aksenov, S.M.; Rusakov, V.S.; Britvin, S.N.; Vozchikova, S.A. Siudaite, $Na_8(Mn^{2+}{}_2Na)Ca_6Fe^{3+}{}_3Zr_3NbSi_{25}O_{74}(OH)_2Cl{\cdot}5H_2O$, a new eudialyte-group mineral from the Khibiny alkaline massif, Kola Peninsula. *Phys. Chem. Miner.* **2018**, *45*, 745–758. [CrossRef]
50. Rastsvetaeva, R.K.; Karipidis, T.K. Cationic ordering in the structure of titanium-rich eudialytes. In Proceedings of the 11th International Conference "Order-Disorder in Minerals and alloys (OMA)", Rostov-on-Don, Russia, 30 September–8 October 2008; Part II. pp. 138–141. (In Russian).
51. Rozenberg, K.A.; Rastsvetaeva, R.K.; Aksenov, S.M. On the centrosymmetric structure of 12-layer eudialytes. In Proceedings of the International Mineralogical Seminar "Mineralogical Intervention into the Micro- and Nanocosm", Syktyvkar, Russia, 9–11 June 2009; pp. 149–151. (In Russian).
52. Rastsvetaeva, R.K.; Rozenberg, K.A.; Khomyakov, A.P. Crystal structure of high-silica K,Na-ordered acentric eudialyte analogue. *Dokl. Chem.* **2009**, *424*, 11–14. [CrossRef]
53. Khomyakov, A.P.; Nechelyustov, G.N.; Rastsvetaeva, R.K.; Rozenberg, K.A. Davinciite, $Na_{12}K_3Ca_6Fe^{2+}{}_3Zr_3(Si_{26}O_{73}OH)Cl_2$, a new K,Na-ordered mineral of the eudialyte group from the Khibiny alkaline massif, Kola Peninsula, Russia. *Geol. Ore Depos.* **2012**, *55*, 532–540. [CrossRef]
54. Khomyakov, A.P.; Nechelyustov, G.N.; Rastsvetaeva, R.K. Aqualite $(H_3O)_8(Na,K,Sr)_5Ca_6Zr_3Si_{26}O_{66}(OH)_9Cl$—A new mineral of eudialyte-group from the alkaline Inagli massif, Saha-Yakutiya, Russia, and oxonium problem in hydrated eudialytes. *Geol. Ore Depos.* **2007**, *136*, 39–55.
55. Rastsvetaeva, R.K.; Viktorova, K.A.; Aksenov, S.M. New data on the Isomorphism in Eudialyte-Group Minerals. II. Refinement of the aqualite crystal structure at 110 K. *Cryst. Rep.* **2018**, *63*, 884–889. [CrossRef]
56. Aksenov, S.M.; Rastsvetaeva, R.K. Refinement of the crystal structure of hyperzirconium eudialyte and its place among low calcium minerals of the eudialyte-group. *Cryst. Rep.* **2013**, *58*, 555–561. [CrossRef]
57. Chukanov, N.V.; Pekov, I.V.; Zadov, A.E.; Korovushkin, V.V.; Ekimenkova, I.A.; Rastsvetaeva, R.K. Ikranite $(Na,H_3O)_{15}(Ca,Mn,REE)_6Fe^{3+}{}_2Zr_3(\square,Zr)(\square,Si)Si_{24}O_{66}(O,OH)_6Cl{\cdot}nH_2O$ and raslakite $Na_{15}Ca_3Fe_3(Na,Zr)_3Zr_3(Si,Nb)(Si_{25}O_{73})(OH,H_2O)_3(Cl,OH)$—New minerals of the eudialyte group from Lovozero massif. *Geol. Ore Depos.* **2003**, *132*, 22–33.
58. Nomura, S.F.; Atencio, D.; Chukanov, N.V.; Rastsvetaeva, R.K.; Coutinho, J.M.V.; Karipidis, T.K. Manganoeudialyte—A new mineral from Poços de Caldas, Minas Gerais, Brazil. *Zapiski Rossiiskogo Mineral. Obshchestva (Proc. Rus. Mineral. Soc.)* **2010**, *139*, 35–47.

59. Zaitsev, V.A.; Aksenov, S.M.; Rastsvetaeva, R.K.; Chukanov, N.V. Sr-rich eudialyte group mineral (Cl-deficient analogue of taseqite) from the Odikhincha Massif, Polar Siberia, Russia. In Proceedings of the XXXIV International Conference "Magmatism of the Earth and Related Strategic Metal Deposits", Miass, Russia, 4–9 August 2017; pp. 319–321.
60. Aksenov, S.M.; Zaitsev, V.A.; Rastsvetaeva, R.K.; Chukanov, N.V. Crystal structure features of Cl-deficient analogue of taseqite from the Odichincha Massif (Russia). *Crystallogr. Rep.* **2018**, *63*, 349–357.
61. Rastsvetaeva, R.K.; Chukanov, N.V.; Zaitsev, B.A.; Aksenov, S.M.; Viktorova, K.A. Crystal structure of Cl-deficiente analog of tasekite from the Odihincha massif. *Cryst. Rep.* **2018**, *63*, 392–400. [CrossRef]
62. Ekimenkova, I.A.; Rastsvetaeva, R.K.; Chukanov, N.V. Crystal structure of the oxonium-containing analogue of eudialyte. *Dokl. Akad. Nauk* **2000**, *371*, 625–628. (In Russian)
63. Rastsvetaeva, R.K.; Chukanov, N.V. Ikranite: Composition and structure of a new mineral of the eudialyte group. *Crystallogr. Rep.* **2003**, *48*, 717–720. [CrossRef]
64. Rozenberg, K.A.; Rastsvetaeva, R.K.; Chukanov, N.V.; Verin, I.A. Crystal structure of a niobium-deficient carbonate analogue of feklichevite. *Doklady Chem.* **2005**, *400*, 25–29. [CrossRef]
65. Giuseppetti, G.; Mazzi, F.; Tadini, C. The crystal structure of eudialyte. *Tshermaks Mineral. Petrogr. Mitt.* **1971**, *16*, 105–127. [CrossRef]
66. Johnsen, O.; Gault, R.A.; Grice, J.D.; Ercit, T.S. Khomyakovite and manganokhomyakovite, two new members of eudialyte group from Mont Saint-Hilaire, Quebec, Canada. *Canad. Mineral.* **1999**, *37*, 893–899.
67. Grice, J.D.; Gault, R.A. Johnsenite-(Ce): A new member of the eudialyte group from Mont Saint-Hilaire, Quebec, Canada. *Canad. Mineral.* **2006**, *44*, 105–115. [CrossRef]
68. Rastsvetaeva, R.K.; Aksenov, S.M.; Chukanov, N.V. Crystal structure of zircono-niobosilicate with Ti-centered Si_9O_{27} rings as a new member of the eudialyte group. *Doklady Phys. Chem.* **2010**, *432*, 106–110. [CrossRef]
69. Rastsvetaeva, R.K.; Chukanov, N.V.; Viktorova, K.A.; Aksenov, S.M. New data on the isomorphism in eudialyte-group minerals. I: Crystal structure of titanium-rich eudialyte from the Kovdor alkaline massif. *Cryst. Rep.* **2018**, *63*, 563–569. [CrossRef]
70. Rastsvetaeva, R.K.; Chukanov, N.V.; Sipavina, L.V.; Voronin, M.V. New data on the isomorphism in eudialyte-group minerals. VIII. Crystal structure of Fe^{2+}-analog of Fe^{2+}-analog feklichevite—Potentionally new mineral from the Khibiny massif. *Cryst. Rep.* **2020**, *65*. in press. [CrossRef]
71. Khomyakov, A.P.; Dusmatov, V.D.; Ferraris, G.; Gula, A.; Ivaldi, G.; Nechelyustov, G.N. Zirsilite-(Ce), $(Na,□)_{12}(Ce,Na)_3Ca_6Mn_3Zr_3Nb[Si_{25}O_{73}](OH)_3(CO_3)·H_2O$, and carbokentbrooksite, $(Na,□)_{12}(Na,Ce)_3Ca_6Mn_3Zr_3Nb[Si_{25}O_{73}](OH)_3(CO_3)·H_2O$, two new eudialyte-group minerals from the Dara-i-Pioz alkaline massif, Tajikistan. *Zapiski Vserossiyskogo Mineral. Obshchestva (Proc. Rus. Mineral. Soc.)* **2003**, *132*, 40–51. (In Russian)
72. Rastsvetaeva, R.K.; Chukanov, N.V.; Pekov, I.V.; Varlamov, D.A.; Aksenov, S.M. New data on the isomorphism in eudialyte-group minerals. VI. Crystal structure of the first member containing sulfide anion with isomorphic substitution Cl^-–S^{2-}. *Cryst. Rep.* **2020**, *65*, 215–222. [CrossRef]
73. Khomyakov, A.P.; Nechelyustov, G.N.; Rastsvetaeva, R.K. Dualite, $Na_{30}(Ca,Na,Ce,Sr)_{12}(Na,Mn,Fe,Ti)_6Zr_3Ti_3Si_51O_{144}(OH,H_2O,Cl)_9$—A new zircono-titanium silicate with modular eudialyte like structure from the Lovozero alkaline massif, Kola peninsula, Russia. *Geol. Ore Depos.* **2007**, *4*, 31–42.
74. Khomyakov, A.P.; Nechelyustov, G.N.; Arakcheeva, A.V. Rastsvetaevite $Na_{27}K_8Ca_{12}Fe_3Zr_6Si_4[Si_3O_9]_4[Si_9O_{27}]_4(O,OH,H_2O)_6Cl_2$—A new mineral with modular eudialyte-like structure and crystal-chemical systematics of eudialyte group. *Geol. Ore Depos.* **2006**, *1*, 49–65.
75. Rastsvetaeva, R.K.; Rozenberg, K.A.; Aksenov, S.M. Modular structure of highly ordered eudialyte and its place among hydrated minerals of rastsvetaevite family. *Cryst. Rep.* **2017**, *62*, 551–557. [CrossRef]
76. Rozenberg, K.A.; Rastsvetaeva, R.K.; Aksenov, S.M. Crystal structure of modular sodium-rich and low-iron eudialyte from Lovozero alkaline massif. *Cryst. Rep.* **2016**, *61*, 779–785. [CrossRef]
77. Khomyakov, A.P.; Nechelyustov, G.N.; Rastsvetaeva, R.K. Labyrinthite $(Na,K,Sr)_{35}Ca_{12}Fe_3Zr_6TiSi_{51}O_{144}(O,OH,H_2O)_9Cl_3$—A new mineral with modular eudialyte-like structure from the Khibiny alkaline massif, Kola peninsula, Russia. *Geol. Ore Depos.* **2006**, *2*, 38–49.
78. Rastsvetaeva, R.K.; Khomyakov, A.P. Modular structure of a high-potassium analog of eudialyte with a doubled period *c*. *Cryst. Rep.* **2001**, *46*, 715–721.

79. Rastsvetaeva, R.K.; Viktorova, K.A.; Aksenov, S.M. New Data on the Isomorphism in Eudialyte-Group Minerals. III. Modular structure of K-analog of centrosymmetrical labyrinthite. *Cryst. Rep.* **2019**, *64*, 203–208. [CrossRef]
80. Pyatenko, J.A.; Kurova, T.A.; Chernitsova, N.M.; Pudovkina, Z.V.; Blinov, V.A.; Maksimova, N.V. *Niobium, Tantalum, and Zirconium in Minerals*; Nauka: Moscow, Russia, 1999; p. 246. (In Russian)
81. Khomyakov, A.P.; Nechelyustov, G.N.; Rastsvetaeva, R.K. Alluaivite, $Na_{19}(Ca,Mn)_6(Ti,Nb)_3Si_{26}O_{74}Cl{\cdot}2H_2O$, a new titanosilicate with a eudialyte-like structure. *Proc. Sov. Mineral. Soc.* **1990**, *119*, 117–120. (In Russian)
82. Johnsen, O.; Grice, J.D.; Gault, R.A. Oneillite: A new Ca-deficient and REE-rich member of the eudialyte group from Mont Saint-Hilaire, Quebec, Canada. *Canad. Mineral.* **1999**, *37*, 1111–1117.
83. Rastsvetaeva, R.K.; Khomyakov, A.P. Crystal structure of a new Mn,Na-ordered analogue of eudialyte with the symmetry *R*3. *Crystallogr. Rep.* **2000**, *45*, 591–594. [CrossRef]
84. Khomyakov, A.P.; Nechelyustov, G.N.; Rastsvetaeva, R.K. Voronkovite, $Na_{15}(Na,Ca,Ce)_3(Mn,Ca)_3Fe_3Zr_3Si_{26}O_{72}(OH,O)_4Cl.H_2O$, a new mineral species of the eudialyte group from the Lovozero alkaline pluton, Kola Peninsula, Russia. *Geol. Ore Depos.* **2009**, *51*, 750–756. [CrossRef]
85. Chukanov, N.V.; Aksenov, S.M.; Pekov, I.V.; Belakovskiy, D.I.; Vozchikova, S.A.; Britvin, S.N. Sergevanite, $Na_{15}(Ca_3Mn_3)(Na_2Fe)Zr_3Si_{26}O_{72}(OH)_3{\cdot}H_2O$, a new eudialyte-group mineral from the Lovozero alkaline massif, Kola Peninsula. *Canad. Mineral.* **2020**, in press. [CrossRef]
86. Rastsvetaeva, R.K.; Rozenberg, K.A.; Pekov, I.V.; Chukanov, N.V.; Möckel, S. Crystal structures of two new low-symmetry calcium-deficient analogs of eudialyte. *Crystallogr. Rep.* **2006**, *51*, 205–211. [CrossRef]
87. Aksenov, S.M.; Rastsvetaeva, R.K. Crystal structure refinement of zirconium rich eudialyte and its place among calcium poor eudialyte group minerals. *Cryst. Rep.* **2013**, *58*, 671–677. [CrossRef]
88. Rastsvetaeva, R.K.; Chukanov, N.V.; Verin, I.A. Crystal structure of hyperzirconium sulfate analogue of eudialyte. *Doklady Earth Sci.* **2006**, *409*, 985–989. [CrossRef]
89. Rastsvetaeva, R.K.; Khomyakov, A.P.; Chizhevskaya, S.V.; Anoprienko, T.V. Ordering in eudialytes with different degree of hydration. In Proceedings of the International Symposium "Phase Conversions in Solid Solutions and Alloys", Sochi, Russia, 4–7 September 2002; pp. 59–62.